

1 Post-mortem molecular profiling of three psychiatric disorders

2
3 Ryne C. Ramaker^{1,2,*}, B.S., Kevin M. Bowling^{1,*}, Ph.D., Brittany N. Lasseigne^{1*}, Ph.D.,
4 Megan H. Hagenauer³, Ph.D., Andrew A. Hardigan^{1,2}, B.S., Nick S. Davis^{1,#}, B.S., Jason
5 Gertz^{1,%}, Ph.D., Preston M. Cartagena⁴, Psy.D., David M. Walsh⁴, Psy.D., Marquis P.
6 Vawter⁴, Ph.D., Edward G. Jones (deceased), M.D., Ph.D., Alan F. Schatzberg⁵, M.D.,
7 Jack D. Barchas⁶, M.D., Ph.D., Stan J. Watson³, M.D., Ph.D., Blynn G. Bunney⁴, Ph.D.,
8 Huda Akil³, Ph.D., William E. Bunney⁴, M.D., Jun Z. Li⁷, Ph.D., Sara J. Cooper¹, Ph.D.,
9 and Richard M. Myers¹, Ph.D.

10 *These authors contributed equally to this study

11 ¹HudsonAlpha Institute for Biotechnology, Huntsville, AL, USA

12 ²Department of Genetics, The University of Alabama at Birmingham, Birmingham, AL,
13 USA

14 ³Mental Health Research Institute, University of Michigan, Ann Arbor, MI, USA

15 ⁴Department of Psychiatry and Human Behavior, College of Medicine, University of
16 California, Irvine, Irvine, CA, USA

17 ⁵Department of Psychiatry, Stanford University School of Medicine, Stanford, CA, USA

18 ⁶Psychiatry, Weill Cornell Medical College, New York, NY, USA

19 ⁷Department of Human Genetics, University of Michigan, Ann Arbor, MI, USA

20

21 Present address:

22 [#]Duke University, Durham, NC, USA

23 [%]University of Utah School of Medicine, Salt Lake City, UT, USA

1

2 To whom correspondence should be addressed:

3 Richard M. Myers, Ph.D.

4 HudsonAlpha Institute for Biotechnology

5 601 Genome Way

6 Huntsville, AL 35806

7 Telephone: 256-327-0431

8 FAX: 256-327-0978

9 rmyers@hudsonalpha.org

10

1 **Abstract**

2 **Background**

3 Psychiatric disorders are multigenic diseases with complex etiology contributing
4 significantly to human morbidity and mortality. Although clinically distinct, several
5 disorders share many symptoms suggesting common underlying molecular changes
6 exist that may implicate important regulators of pathogenesis and new therapeutic
7 targets.

8 **Results**

9 We compared molecular signatures across brain regions and disorders in the
10 transcriptomes of postmortem human brain samples. We performed RNA sequencing
11 on tissue from the anterior cingulate cortex, dorsolateral prefrontal cortex, and nucleus
12 accumbens from three groups of 24 patients each diagnosed with schizophrenia, bipolar
13 disorder, or major depressive disorder, and from 24 control subjects, and validated the
14 results in an independent cohort. The most significant disease differences were in the
15 anterior cingulate cortex of schizophrenia samples compared to controls. Transcriptional
16 changes were assessed in an independent cohort, revealing the transcription factor
17 *EGR1* as significantly down regulated in both cohorts and as a potential regulator of
18 broader transcription changes observed in schizophrenia patients. Additionally, broad
19 down regulation of genes specific to neurons and concordant up regulation of genes
20 specific to astrocytes was observed in SZ and BPD patients relative to controls. We also
21 assessed the biochemical consequences of gene expression changes with untargeted
22 metabolomic profiling and identified disruption of GABA levels in schizophrenia patients.

1 **Conclusions**

2 We provide a comprehensive post-mortem transcriptome profile of three psychiatric
3 disorders across three brain regions. We highlight a high-confidence set of
4 independently validated genes differentially expressed between schizophrenia and
5 control patients in the anterior cingulate cortex and integrate transcriptional changes
6 with untargeted metabolite profiling.

7 **Keywords**

8 Schizophrenia, Bipolar Disorder, Major Depressive Disorder, RNA sequencing,
9 metabolomics, *EGR1*

10 **Background**

11 Schizophrenia (SZ), bipolar disorder (BPD), and major depressive disorder (MDD) are
12 multigenic diseases with complex etiology and are large sources of morbidity and
13 mortality in the population. All three disorders are associated with high rates of suicide,
14 with ~90% of the ~41,000 people who commit suicide each year in the U.S. having a
15 diagnosable psychiatric disorder [1]. Notably, while clinically distinct, these disorders
16 also share many symptoms, including psychosis, suicidal ideation, sleep disturbances
17 and cognitive deficits [2–4]. This phenotypic overlap suggests potential common genetic
18 etiology, which is supported by recent large-scale genome-wide association studies [5–
19 8]. However, this overlap has not been fully characterized with functional genomic
20 approaches. Current therapies for these psychiatric disorders are ineffective in many
21 patients and often only treat a subset of an individual patient’s symptoms [9].
22 Approaches targeting the underlying molecular pathologies within and across these

1 types of disorders are necessary to address the immense burden of psychiatric disease
2 around the world and improve care for the millions of people diagnosed with these
3 conditions.

4 Previous studies [10–14] analyzed brain tissue with RNA sequencing (RNA-seq) in SZ
5 and BPD, and identified altered expression of GABA-related genes in the superior
6 temporal gyrus and hippocampus, as well as differentially expressed genes related to
7 neuroplasticity and mammalian circadian rhythms. Our study focused on the anterior
8 cingulate cortex (AnCg), dorsolateral prefrontal cortex (DLPFC), and nucleus
9 accumbens (nAcc), regions which are often associated with mood alterations, cognition,
10 impulse control, motivation, reward, and pleasure – all behaviors known to be altered in
11 psychiatric disorders [15,16]. To assess gene expression changes associated with
12 psychiatric disease in these three brain regions, we performed RNA-seq on macro-
13 dissected post-mortem tissues in four well-documented cohorts of 24 patients each with
14 SZ, BPD, MDD and 24 controls (CTL) (96 individuals total). Additionally, we conducted
15 metabolomic profiling of AnCg tissue from the same subjects. RNA-seq analysis
16 revealed common expression profiles in SZ and BPD patients supporting the notion that
17 these disorders share a common molecular signature. Transcriptional changes were
18 most pronounced in the AnCg with SZ and BPD exhibiting strongly correlated
19 differences from CTL samples. Differentially expressed genes were associated with cell-
20 type composition with BPD and SZ samples showing decreased expression of neuron-
21 specific genes. We validated this result with RNA-seq data from an independent cohort
22 of 35 cases each of SZ, BPD, and CTL post-mortem cingulate cortex samples from the
23 Stanley Neuropathology Consortium Integrative Database (SNCID;

1 <http://sncid.stanleyresearch.org>) Array Collection. We present a set of validated genes
2 differentially expressed between SZ and CTL patients, perform an integrated analysis of
3 metabolic pathway disruptions, and highlight a role for the transcription factor, *EGR1*,
4 whose down-regulation in SZ patients may drive a large portion of observed
5 transcription changes.

6 **Methods**

7 See Supplemental Methods for additional detail.

8 **Patient Sample Collection and Preparation**

9 Sample collection, including human subject recruitment and characterization, tissue
10 dissection, and RNA extraction, was described previously [17,18] as part of the Brain
11 Donor Program at the University of California, Irvine, Department of Psychiatry and
12 Human Behavior (Pritzker Neuropsychiatric Disorders Research Consortium) under IRB
13 approval. In brief, coronal slices of the brain were rapidly frozen on aluminum plates that
14 were previously frozen to -120°C and dissected as described previously [19]. All
15 samples were diagnosed by psychological autopsy, which included collection and
16 analyses of medical and psychiatric records, toxicology, medical examiners' reports,
17 and 141-item family interviews. Agonal state scores were assigned based on a
18 previously published scale [20]. Controls were selected based upon absence of severe
19 psychiatric disturbance and mental illness within first-degree relatives.

20 We obtained fastq files from RNA-seq experiments for our validation cohort from the
21 Stanley Neuropathology Consortium Integrative Database (SNCID;
22 <http://sncid.stanleyresearch.org>) Array Collection comprising 35 cases each of SZ, BPD,

1 and CTL of post-mortem cingulate cortex with permission on June 30, 2015. For our
2 analysis, we included the 27 SZ, 26 CTL, and 25 BPD SNCID samples that were
3 successfully downloaded and represented unique samples. SNCID RNA-seq
4 methodology and data processing are described in detail in a previous publication that
5 makes use of the data [10].

6 **RNA-seq and Data Processing**

7 To extract nucleic acid, 20 mg of post-mortem brain tissue was homogenized in Qiagen
8 RLT buffer + 1% BME using an MP FastPrep-24 and Lysing Matrix D beads for three
9 rounds of 45 seconds at 6.5 m/s (FastPrep homogenizer, lysing matrix D, MP Bio). Total
10 RNA was isolated from 350 μ L tissue homogenate using the Norgen Animal Tissue
11 RNA Purification Kit (Norgen Biotek Corporation). We made RNA-seq libraries from 250
12 ng total RNA using polyA selection (Dynabeads mRNA DIRECT kit, Life Technologies)
13 and transposase-based non-stranded library construction (Tn-RNA-seq) as described
14 previously [21]. To mitigate potentially confounding batch effects in sample preparation
15 we randomly assigned samples from all brain regions and disorders into batches of 24
16 samples. We used KAPA to quantitate the library concentrations and pooled 4 samples
17 in order to achieve equal concentration of the four libraries in each lane. Pools were
18 determined by random from the 291 samples. Samples were also randomly selected for
19 pooling in an effort to limit potentially confounding sequencing batch effects. The pooled
20 libraries were sequenced on an Illumina HiSeq 2000 sequencing machine using paired-
21 end 50 bp reads and a 6 bp index read, resulting in an average of 48.2 million reads per
22 library. To quantify the expression of each gene in both Pritzker and SNCID datasets,
23 RNA-seq reads were processed with aRNApipe v1.1 using default settings [22]. Briefly,

1 reads were aligned and counted with STAR v2.4.2a to all genes annotated in
2 GRCh37_E75 [23]. All alignment quality metrics were obtained from the picard tools
3 module (<http://broadinstitute.github.io/picard/>) available in aRNApipe. Genes expressed
4 from the X and Y chromosomes were omitted from the study.

5 Quantitative PCR (qPCR) was performed on 10 SZ and 10 CTL patients to validate
6 *EGR1* RNA-seq measurements. RNA was extracted as described above from tissue
7 lysates a second time. Reverse transcription was performed on 250ng of input RNA with
8 the Applied Biosystems high capacity cDNA reverse transcription kit. Validated Taqman
9 assays for *EGR1* (Hs00152928_m1) and the housekeeper genes *GAPDH*
10 (Hs02758991_g1) and *ACTB* (Hs01060665_g1) were used for qPCR. cDNA was
11 diluted by a factor of 10 before use as input for the Taqman assay. The qPCR
12 reaction was performed on an Applied Biosystems Quant Studio 6 Flex system
13 using the recommended amplification protocol for Taqman assays.

14 **Sequencing Data Analysis**

15 All data analysis in R was performed with version 3.1.2.

16 *Differential Expression Analysis and Normalization*

17 To examine gene expression changes, we employed the R package DESeq2 [24]
18 (version 1.6.3), using default settings, but employing likelihood ratio test (LRT)
19 hypothesis testing, and removing non-convergent genes from subsequent analysis.
20 Genes differentially expressed between each disorder and CTL samples, by brain
21 region, were identified with DESeq2 (adjusted p-value<0.05), including age, brain pH,
22 PMI, and percentage of reads uniquely aligned (PRUA) as covariates (Full Model:

1 ~Age+PMI+pH+PRUA+Disorder, Reduced Model: ~ Age+PMI+pH+PRUA). For
2 downstream heatmap visualization, PCA, and cell-type analysis, genes underwent a
3 log-like normalization using DESeq2's varianceStabilizingTransformation function and
4 were corrected for PRUA by computing residuals to a linear model regressing PRUA on
5 normalized gene expression level with the R lm function unless otherwise specified.
6 DESeq2's default independent filtering method was used to remove genes with an
7 insufficient expression level from further analysis.

8 *PCA and Hierarchical Clustering*

9 PCA analysis was performed in R on normalized data using the prcomp() command.
10 Hierarchical clustering of normalized gene expression data was done in R with the
11 hclust command (method="ward", distance="Euclidean")

12 *Pathway Enrichment Analysis*

13 Pathway analysis was conducted using the web-based tool LRPath [25] using all GO
14 term annotations, adjusting to gene read count with RNA-Enrich, including directionality
15 and limiting maximum GO term size to 500 genes. GO term visualization was performed
16 using the Cytoscape Enrichment Map plug-in [26]. The Genesetfile (.gmt) GO
17 annotations from February 1, 2017 were downloaded from
18 http://download.baderlab.org/EM_Genesets/. The LRPath output was parsed and used
19 as an enrichment file with all upregulated pathways colored red and all downregulated
20 pathways colored blue, regardless of degree of upregulation. Mapping parameters
21 were; p-value cutoff = 0.005, FDR cutoff = 0.1 and Jaccard coefficient > 0.3. Resulting
22 networks were exported as PDFs. Summary terms were added to the plot based on the
23 GO terms in those clusters. In order to assess overlap between significant GO terms in

1 our analysis and the GWAS study described by the Psychiatric Genomics Consortium,
2 we downloaded the p-values reported for Schizophrenia hits from their Supplemental
3 Table 4, which contained 424 significant GO terms. We used a chi-squared test to
4 assess significant overlap between the two groups. Our Supplemental Table 5 reports
5 the p-values measured in SZ based on this study along with those calculated in our
6 analysis.

7 *EGR1 ChIP-seq peak analysis*

8 Narrow peak bed files filtered to optimal IDR peaks were obtained from the ENCODE
9 data portal (www.encodeproject.org) for *EGR1* ChIP-seq data in GM12878, H1-hESC,
10 and K562 cell lines (ENCODE file IDs: ENCFF002CIV, ENCFF002CGW,
11 ENCFF002CLV). Consensus *EGR1* peaks were identified by intersecting peaks from all
12 three cell lines, which resulted in a final list of 4,121 peaks common to all cell lines
13 (minimum overlap of 1 bp). The distance from each annotated transcription start site
14 (TSS) to the nearest consensus *EGR1* peak was computed based on TSSs annotated
15 in the ENSEMBL gene transfer format (GTF) file from the Ensembl data release 75
16 (GRCh37_E75).

17 *Cell-Specific Enrichment Analysis*

18 Sets of genes uniquely expressed by several brain cell-types were obtained from figure
19 1B in Darmanis et. al [27]. An index for each cell-type was created by calculating the
20 median normalized expression value for each set of cell-type associated genes. Index
21 values were compared across patient clusters by non-parametric rank sum tests and
22 spearman correlation with top principal components. To validate our method, we
23 calculated cell-type specific indices from an independent cohort of previously published

1 purified brain cells [28,29]. FPKM-normalized gene expression data was obtained from
2 supplemental table 4 of Zhang et. al. (2014) and cell-type indexes were calculated as
3 described above. To examine index performance in mixed cell populations, we obtained
4 fastq files for neuron and astrocyte-purified brain samples from GEO accession
5 GSE73721 and generated raw count files as described above. We next mixed
6 expression profiles *in silico* by performing random down-sampling of neuron and
7 astrocyte count levels and summing the results such that mixed populations containing
8 specific proportions of counts from neuron- and astrocyte-purified tissue were
9 generated. For example, to generate an 80/20 neuron to astrocyte mixture, neuron and
10 astrocyte count columns (which started at an equivalent number of 5,759,178 aligned
11 reads) were randomly down-sampled to 4,607,342 and 1,151,836 counts respectively
12 and summed across each gene to result in a proportionately mixed population of
13 aligned count data simulating heterogeneous tissue. Then we calculated a
14 neuron/astrocyte index ratio capable of predicting the *in silico* mixing weights. Briefly,
15 we assumed index values for mixed cell populations were directly proportional to mixing
16 weights of their respective purified tissue, thus the predicted cell proportion for a given
17 cell type was simply calculated as:

18
$$\text{predicted cell proportion} = \text{observed index value} / \text{purified tissue index value}$$

19 To insure cell-type predictive power was unique to indices derived from Darmanis et. al
20 genes, we generated indices from 10,000 randomly sampled gene sets of equivalent
21 size and examined their performance in predicting *in silico* mixing weights. Mean
22 squared prediction errors (MSE) were calculated for each of the 10,000 null indices and
23 compared to the MSE of Darmanis et. al.-derived indices.

1 Cell type deconvolution analysis was confirmed using a previously published algorithm
2 implemented in the R package deconRNAseq [30]. The “datasets” input to the
3 deconRNAseq function was a normalized count matrix of all AnCg brain samples and
4 the “signatures” input consisted of a normalized count matrix of astrocyte, neuron,
5 microglia, and oligodendrocyte dissected cells from the GEO accession GSE73721
6 previously described.

7 Enrichment analysis for extreme fold change was performed by randomly sampling the
8 fold changes of 1000 null gene sets equivalent in size and expression level (allowing
9 5% error) to the neuron and astrocyte specific gene sets. The median fold change of
10 each 1000 null gene set was compared to the observed median fold change for neuron
11 and astrocyte gene sets respectively.

12 **Metabolomics**

13 *Sample preparation*

14 Sections of approximately 100mg of frozen tissue were weighed and homogenized for
15 45 seconds at 6.5M/s with ceramic beads in 1mL of 50% methanol using the MP
16 FastPrep-24 homogenizer (MP Biomedicals). A sample volume equivalent to 10mg of
17 initial tissue weight was dried down at 55°C for 60 minutes using a vacuum concentrator
18 system (Labconco). Derivatization by methoximation and trimethylsilylation was done as
19 previously described [31].

20 We analyzed technical replicates of each tissue sample, in randomized order.

21 *GCxGC-TOFMS analysis*

1 All derivatized samples were analyzed on a Leco Pegasus 4D system (GCxGC-
2 TOFMS), controlled by the ChromaTof software (Leco, St. Joseph, MI). Samples were
3 analyzed as described previously [31] with minor modifications in temperature ramp.

4 *Data analysis and metabolite identification*

5 Peak calling, deconvolution and library spectral matching were done using ChromaTOF
6 4.5 software. Peaks were identified by spectral match using the NIST, GOLM [32], and
7 Fiehn libraries (Leco), and confirmed by running derivatized standards (Sigma). We
8 used Guineu for multiple sample alignment [33].

9 *Integrated Pathway Analysis*

10 Altered metabolites and genes were analyzed for enrichment in KEGG pathways
11 containing both metabolite and gene features. A non-parametric, threshold free pathway
12 analysis similar to that of a previously described method [34] was first performed on
13 metabolite and gene expression data separately. Our method builds on the principle
14 described by Subramanian that implements a one-tailed Wilcox test to identify pathways
15 enriched for low p-values. Instead of just accounting for enrichment at the gene level,
16 we use metabolite or gene p-value ranks within each pathway compared to remaining
17 non-pathway metabolites or genes with a one-tailed Wilcox test to test the hypothesis
18 that elements of a given pathway may be enriched for lower p-value ranks than
19 background elements. Metabolite and gene p-values were subsequently combined to
20 provide an integrated enrichment significance p-value using Fisher's method. Pathways
21 had to contain greater than 5 genes and 1 metabolite measured in our dataset to be
22 included in the analysis. Table 10 lists p-values for enriched pathways based on genes,
23 metabolites or combined.

1 **Results**

2 **Region-specific gene expression in control and psychiatric brain tissue**

3 We collected post-mortem human brain tissue, associated clinical data, including age,
4 sex, brain pH, and post-mortem interval (PMI), and cytotoxicology results (Tables S1-2)
5 for matched cohorts of 24 patients each diagnosed with SZ, BPD, or MDD, as well as
6 24 control individuals with no personal history of, or first-degree relatives diagnosed
7 with, psychiatric disorders. Importantly, to limit the effect of acute patient stress at the
8 time of death as a potential confounder we included only patients with an agonal factor
9 score of zero and a minimum brain pH of 6.5 [18]. Using RNA-seq [21], we profiled gene
10 expression in three macro-dissected brain regions (AnCg, DLPFC, nAcc). After quality
11 control, we analyzed 57,905 ENSEMBL genes in a total of 281 brain samples (Table
12 S3).

13 To examine heterogeneity across brain regions and subjects, we performed a principal
14 component analysis (PCA; Figure S1A) of all genes. The first principal component
15 (PC1, 21.8% of the variation) separates cortical AnCg and DLPFC samples from
16 subcortical nAcc samples. Examination of the first and second principal components for
17 disorder associations reveals a separation of some SZ and BPD samples from all other
18 samples (Figures S1B and S2A-C). However, in agreement with previously reported
19 post-mortem brain RNA sequencing studies [14], we found several principal
20 components to be highly correlated with quality metrics including the percentage of
21 reads uniquely aligned and percentage of reads aligned to mitochondrial sequence
22 (absolute $Rho > 0.5$, $FDR < 1E-16$, Table S4). To reduce the potentially confounding
23 effects of sample quality, we repeated the PCA on expression data normalized to the

1 percentage of reads uniquely aligned for each sample and found that global disease-
2 specific expression differences were significantly reduced and PC1 primarily separated
3 nAcc samples from AnCg and DLPFC brain regions (Figures S1C and S2D-I).

4 **Disease-specific gene expression in control and psychiatric brains**

5 We next applied DESeq2 [24], a method for analyzing differential sequence read count
6 data, to identify genes differentially expressed across disorders within each brain region
7 after correcting for biological and technical covariates. The largest number of significant
8 expression changes occurred in AnCg between SZ and CTL individuals (87 genes,
9 FDR<0.05, Figure 1A). Pathway enrichment analysis of differentially expressed genes
10 between SZ and CTL patients revealed 935 gene ontology (GO) terms with an
11 FDR<0.05 (Table S5) (122 GOCC, 159 GOMF, and 654 GOBP). Significant GO terms
12 fall into the broad categories of synaptic function and signaling (e.g. neurotransmitter
13 transport, ion transport, calcium signaling) (Figure S3). These terms overlap significantly
14 with those identified by the Psychiatric Genomics Consortium in their analysis of GWAS
15 implicated genes [35] with 68 GO terms meeting a p-value cutoff of <0.05 in both
16 datasets (p-value<0.0001, Chi-square test). Additionally, nine genes were differentially
17 expressed between SZ and CTL individuals in DLPFC. Three of these were also
18 identified in AnCg: *SST*, *PDPK2P* and *KLHL14*. No genes had an FDR<0.05 when
19 comparing BPD or MDD samples to CTLs in any brain region, or comparing SZ and
20 CTL tissues in nAcc (Table S6). To examine potential common gene expression
21 patterns between the psychiatric disorders, we performed pair-wise correlation
22 calculations of all gene log₂ fold changes for each disorder versus controls in each brain
23 region. Of the nine case-control comparisons (for three regions and three diseases), a

1 particularly strong correlation is observed between BPD and SZ compared to either SZ
2 or BPD and MDD in each brain region (Figure 1B). In the AnCg, BPD and SZ share
3 1,020 common genes differentially expressed at an uncorrected DESeq2 p -value <0.05
4 compared to only 248 and 143 genes shared between MDD and SZ or BPD
5 respectively (Figure 1C). This strong overlap between BPD and SZ (Fisher's exact p -
6 value $<1E-16$) indicates that although expression changes are weaker in BPD they
7 follow a trend similar to those identified in SZ.

8 Because previous post-mortem analyses have been limited by, and are particularly
9 vulnerable to, biases inherent to examining a single patient cohort, we sought to
10 generate a robust set of SZ associated genes by validating our observed expression
11 changes in an independent cohort. To accomplish this, we examined gene expression
12 differences in the AnCg between SZ and CTL samples in the SNCID RNA-seq Array
13 dataset [13], revealing 1,003 genes altered (DESeq2 uncorrected p -value <0.05) in both
14 datasets (Fisher's p -value $<1E-16$, Table S7). The magnitude and direction of change in
15 significant genes in the Pritzker dataset were highly correlated with the SNCID dataset
16 ($Rho=0.202$, p -value $<1E-16$), particularly in 87 genes that met a cutoff of $FDR<0.05$
17 ($Rho=0.812$, p -value $<1E-16$; Figure 1D). We performed hierarchical clustering of SZ
18 and CTL samples in the SNCID validation cohort using the 1,003 genes differentially
19 expressed, at the less stringent threshold, p -value <0.05 , between SZ and CTL in the
20 Pritzker dataset (Figure 1E), and found these genes successfully distinguished the two
21 disease groups with only 5 out of 27 SZ and 2 out of 26 CTL samples misclassified.
22 Of particular interest are the 5 genes significant at a $FDR<0.05$ in both cohorts including
23 a nearly 2-fold decrease in expression of the transcription factor *EGR1* (Table S7A,

1 Figure 2A). Quantitative PCR (qPCR) validation confirmed reduced *EGR1* expression in
2 SZ samples (Figure 2B, Wilcox p-value=4.33x10E-5). *EGR1*, a zinc finger transcription
3 factor, has been recently implicated in SZ by a GWAS study [5], thus we sought to
4 investigate whether loss of *EGR1* expression might be associated with transcriptional
5 changes observed in the AnCg of SZ patients using publicly available genome-wide
6 occupancy data from the ENCODE consortium (<https://www.encodeproject.org>). To
7 obtain high confidence *EGR1* binding sites we intersected chromatin
8 immunoprecipitation sequencing (ChIP-Seq) peaks derived from the H1-hESC, K562,
9 and GM12878 cell lines. We found that genes with a transcription start site (TSS) within
10 1kb of an *EGR1* binding site had significantly lower DESeq2 p-values (Wilcox p-
11 value=9.68E-5) and reduced expression in SZ versus CTL (Wilcox p-value=7.69E-15)
12 compared to genes whose TSSs were greater than 1kb from an *EGR1* binding site. A
13 monotonic decrease in this effect was observed as the distance threshold used for this
14 comparison was increased from 1kb to 50kb (Figure 2C).

15 **Cell type specific changes**

16 In addition to dysregulation of broadly acting transcription factors, another mechanism
17 that can drive large-scale transcriptional changes in bulk tissue is alterations in
18 constituent cell type proportions. Previous studies have observed decreases in neuron
19 density and increased glial scarring in psychiatric disorders [36,37]. To test for signs of
20 changing cell populations in our dataset we applied a method to deconvolute RNA
21 expression data and estimate cell type proportions. Darmanis et al. identified genes
22 capable of classifying cells into the major neuronal, glial, and vascular cell-types in the
23 brain based on single cell RNA sequencing. We used these gene sets to generate cell

1 type indices using the median of normalized counts for each cell type-specific gene set.
2 We tested these indices on purified brain cell populations (Zhang et al.) and *in silico*
3 mixed cell populations to demonstrate their accuracy and specificity [28,29] (Figure S4).
4 Application of these cell type indices to patient AnCg expression data revealed a
5 significant decrease in neuron specific gene expression (Wilcox p-value<0.05) and a
6 significant increase in astrocyte specific expression (Wilcox p-value<0.05) in SZ and
7 BPD patients compared to controls (Figures 3A-B). Other brain cell-type indices were
8 not significantly different between psychiatric patients and controls (Figure S5). An
9 alternate algorithm for cell type deconvolution, DeconRNASeq, showed similar results
10 (Figure S6A,B).

11 Additionally, we showed that neuron-specific genes identified by Darmanis et al. are
12 enriched for decreased expression in SZ compared to controls and astrocyte-specific
13 genes are enriched for increased expression (Figure S6C). Again, these enrichments
14 are specific to this gene set and are not reproduced by 1000 expression matched,
15 randomly sampled gene sets (Figure S6D,E). Further supporting a decrease in neuronal
16 gene expression, we found a significant negative correlation between gene expression
17 changes in patient brains relative to control brains and the degree of neuron specific
18 transcription (fold enrichment of neuronal gene expression over other cell types) (SZ
19 $Rho=-0.50$ and BPD $Rho=-0.41$, p-value<1E-16, SZ shown in Figure 3C).

20 **Transcriptomic changes reflected in altered metabolomic profiles**

21 To assess the biochemical consequences of expression changes, we used 2D-GCMS
22 to measure metabolite levels in 86 of the AnCg samples (sufficient tissue was
23 unavailable for 10 samples). We measured and identified 141 unique metabolites (Table

1 S8). We found no metabolites reached statistical significance (FDR<0.05), however 8
2 metabolites had an FDR<0.1 when comparing SZ to CTL. Similar to our gene
3 expression analysis, metabolite levels (Table S9) successfully differentiated SZ and
4 BPD patients from CTLs (Figure 4A), while MDD metabolite profiles were very similar to
5 CTLs. Several of the most significant metabolites, including GABA, are known to be
6 relevant to BPD and SZ (Figure 4B) [38]. Furthermore, GABA/glutamate metabolite
7 ratios correlate strongly with average *GAD1* and *GAD2* expression levels measured by
8 RNA-seq (Rho = 0.413, p-value=0.007, Figures 4C-D). This metabolite-gene
9 relationship is consistent with previous multi-level phenomic analyses [39] and
10 demonstrates realized biochemical consequences from altered gene expression.
11 Notably, reductions in GABA could coincide with loss of neuron specific gene
12 expression as suggested by the RNA-seq data. Integrated pathway analyses of
13 metabolite and gene expression data revealed disruption of synaptic and
14 neurotransmitter signaling in SZ compared to CTL (Figure S7, Table S10).

15 **Discussion**

16 Here, we describe a large transcriptomic dataset across three brain regions (DLPFC,
17 AnCg, and nAcc) in SZ, BPD, and MDD patients, as well as CTL samples matched for
18 agonal state and brain pH. In MDD, we do not identify any genes that meet genome-
19 wide significance for differential expression between cases and controls in any brain
20 region. This finding agrees with previous post-mortem RNA-seq studies [40], however
21 sample size and the choice of brain regions examined likely contributed to our inability
22 to replicate results from previous non-transcriptome wide sequencing based
23 approaches comparing MDD to CTL in post-mortem brain [41]. One limitation of our

1 study is that females are underrepresented at a rate of about 5:1. This reflects the
2 increased chance of accidental death among males [42], but limits us in our ability to
3 make more general conclusions about these disorders and to address known
4 differences between the sexes as they relate to these disorders. We also do not have
5 information on the smoking status for our cohort, which is an important covariate as
6 smoking rates are higher among patients with psychiatric disorders and smoking has
7 been demonstrated to effect gene expression [43,44]. Another potential limitation
8 inherent to post-mortem cohort analyses is accounting for patient drug use. As detailed
9 in Table S2, patient toxicology reports were positive for several prescribed and illicit
10 drugs that were not present in CTL samples. As this is a bias inherent to psychiatric
11 patients it is impossible to disentangle from non-treatment related disease patterns in a
12 post-mortem analysis.

13 Another important limitation of post-mortem RNA-sequencing studies is RNA quality.
14 We found a significant proportion of variation in our data to be associated with multiple
15 alignment quality metrics. Significant effort went into controlling for potential sources of
16 bias due to differences in RNA quality. We only included tissue from patients with an
17 agonal score of 0 and who had a brain pH of 6.5 or greater. We also controlled for brain
18 pH, post-mortem interval, and alignment quality in all differential expression analyses.
19 Our study, as well as future post-mortem studies, could be improved by directly
20 measuring RNA quality at the time of sample preparation (e.g. RNA integrity number
21 (RIN)). Even with these caveats, we believe our data yield new insights contributing to a
22 growing understanding of these disorders.

1 The most dramatic gene expression signals we observed were brain region-specific.
2 The majority of disease-associated expression differences were seen in the AnCg of SZ
3 compared to CTL individuals. The AnCg has been associated with multiple disease-
4 relevant functions, including cognition, error detection, conflict resolution, motivation,
5 and modulation of emotion [45–47]. We observed a striking overlap in SZ- and BPD-
6 associated expression changes consistent with previous findings [38,48].

7 One of the more intriguing genes significantly down regulated ($FDR < 0.05$) in both
8 cohorts of SZ patients was the zinc finger transcription factor, *EGR1*. We provide
9 evidence that this factor binds upstream of a genes with altered expression in SZ and
10 are associated with decreased expression in SZ patients. Down regulation of *EGR1* has
11 been previously described in the prefrontal cortex of post-mortem brain samples from
12 SZ patients [49,50]. *EGR1* has also previously been associated with several
13 phenotypes relevant to psychiatric disorder including neural differentiation [51],
14 emotional memory formation [52], response to antipsychotics [53], and has recently
15 been described as part of a transcription factor-miRNA co-regulatory network capable of
16 acting as a biomarker in peripheral blood cells (PBCs) for SZ [54]. In mice, loss of
17 *EGR1* has linked to neuronal loss in a model of Alzheimer’s Disease [55]. *EGR1* is also
18 important for regulation of the NMDA Receptor pathway, which is critical for synaptic
19 plasticity and memory formation and has been implicated in SZ in humans [56]. We
20 believe a more detailed examination of genome-wide *EGR1* occupancy in post-mortem
21 brain tissue or cultured neurons could yield additional information and assessment of
22 the functional consequences of *EGR1* perturbation is required to confirm this factor’s
23 role in SZ pathogenesis.

1 We also see evidence for depletion of neuron-specific genes and increased levels of
2 astrocyte-specific genes in SZ and BPD patients. This observation is further supported
3 by metabolomic analysis of the AnCg, which found a concordant decrease in GABA
4 levels in BPD and SZ individuals. Neuronal depletion has been previously described in
5 SZ [36,37]. Insufficient tissue remains from our patient cohort to validate computational
6 cell type predictions immunohistochemically, however our data strongly suggests that
7 future post-mortem studies should be cognizant of cell type heterogeneity across patient
8 samples. The method for cell type composition estimation is limited in its accuracy to
9 estimating only the major classes of cells present. Genes represented in cell types
10 present at only a small minority could be over or under-represented using this
11 technique. Based on these results, future studies should consider using robust
12 techniques for assessing tissue composition to examine potential cell type proportion
13 differences between disease cohorts and to identify which transcriptional changes occur
14 in conjunction with, and independent of, those differences.

15 We observed very few or no significant expression differences in the DLPFC and nAcc,
16 which contradicts several previous studies [57,58]. We do not intend to claim that no
17 transcriptional changes occur in these brain regions as our study was designed to
18 broadly compare transcriptional alterations across multiple brain regions in multiple
19 psychiatric disorders, thereby sacrificing exceptional sample sizes in any single disorder
20 in any specific brain region. However, our data does suggest that of the regions we
21 tested, the strongest transcriptional changes occur in the AnCg of SZ patients.
22 Moreover, this data provides a useful resource for future studies facilitating the testing
23 of preliminary hypotheses or validation of significant findings.

1 **Conclusions**

2 Our study provides several meaningful and novel contributions to the understanding of
3 psychiatric disease. We provide a well-annotated data set that has the potential to act
4 as a broadly applicable resource to investigators interested in molecular changes in
5 multiple psychiatric disorders across multiple brain regions. We have conducted an
6 extensive characterization of the molecular overlap between SZ and BPD at the gene
7 expression and metabolite level across multiple brain regions. We provide a high
8 confidence set of genes differentially expressed between SZ and CTL individuals
9 utilizing two independent cohorts and highlight down regulation of *EGR1* as a potential
10 driver of broader scale transcription changes. We also establish that a significant
11 proportion of transcriptome variation within SZ and BPD cohorts is correlated with
12 expression changes in previously identified cell type-specific genes.

13 **List of abbreviations**

14 RNA-seq – RNA sequencing
15 GABA – gamma-Aminobutyric acid
16 GWAS – genome-wide association study
17 SZ – schizophrenia
18 BPD – bipolar disorder
19 MDD – major depression disorder
20 CTL – control
21 AnCg – anterior cingulate gyrus

- 1 DLPFC – dorsolateral prefrontal cortex
- 2 nAcc – nucleus accumbens
- 3 GO – gene ontology
- 4 ChIP-seq – chromatin immunoprecipitation with DNA sequencing
- 5 PCA – principal component analysis

6 **Declarations**

7 **Ethics approval and consent to participate**

8 Sample collection, including human subject recruitment and characterization, was
9 conducted as part of the Brain Donor Program at the University of California, Irvine,
10 Department of Psychiatry and Human Behavior (Pritzker Neuropsychiatric Disorders
11 Research Consortium) under IRB approval (UCI 88-041, UCI 97-74).

12 **Consent for publication**

13 Not applicable

14 **Availability of data and materials**

15 The datasets supporting the conclusions of this article are available in the GEO
16 repository, GSE80655.

17 **Competing interests**

18 The authors declare that they have no competing interests.

19 **Funding**

20 The Pritzker Neuropsychiatric Disorders Research Fund L.L.C. and the NIH-National

1 Institute of General Medical Sciences Medical Scientist Training Program
2 (5T32GM008361-21) supported this work.

3 **Author's Contributions**

4 HA, SJW, AFS, WEB, JDB, HK, SJC and RMM conceived of study

5 KMB, RCR, BNL, SJC, AAH, MH, JZL and RMM designed the experiments

6 EGJ performed brain dissections

7 PMC procured the brain tissue samples

8 MPV analyzed pH on all cases and matched the 4 cohorts

9 DWM obtained demographic and clinical data on all subjects through analyses of
10 medical records and next-of-kin interviews

11 NSD, JG, and KMB collected RNAs and performed Tn-RNA-seq library construction

12 RCR and BNL analyzed the RNA-seq data

13 RCR and SJC performed and analyzed metabolomics experiments

14 KMB, RCR, and BNL wrote the first draft of the paper

15 JZL, BGB, WEB, SJW, SJC, HA and RMM contributed to the writing of the paper

16 All authors read and approved the final manuscript.

17 **Acknowledgements**

18 We thank Marie Kirby, Brian Roberts, Mark Mackiewicz, and Greg Cooper for many
19 helpful discussions and comments on the manuscript, and all the members of the
20 Pritzker Neuropsychiatric Disorders Consortium for their support and advice.

1 **References**

- 2 1. CDC Burden of Mental Illness. 2015.
- 3 2. DSM-5. Diagnostic and Statistical Manual. 2013.
- 4 3. Caldwell CB, Gottesman II. Schizophrenics kill themselves too: a review of risk
5 factors for suicide. *Schizophr. Bull.* 1990;16:571–89.
- 6 4. Siris SG. Suicide and schizophrenia. *J. Psychopharmacol.* [Internet]. 2001 [cited
7 2017 Feb 16];15:127–35. Available from:
8 <http://jop.sagepub.com/cgi/doi/10.1177/026988110101500209>
- 9 5. Ripke S, Neale BM, Corvin A, Walters JTR, Farh K-H, Holmans P a., et al. Biological
10 insights from 108 schizophrenia-associated genetic loci. *Nature* [Internet].
11 2014;511:421–7. Available from: <http://www.nature.com/doi/10.1038/nature13595>
- 12 6. Purcell SM, Wray NR, Stone JL, Visscher PM, O'Donovan MC, Sullivan PF, et al.
13 Common polygenic variation contributes to risk of schizophrenia and bipolar disorder.
14 *Nature.* 2009;460:748–52.
- 15 7. Cross-disorder Psychiatric Genomics Group. Identification of risk loci with shared
16 effects on five major psychiatric disorders: a genome-wide analysis. *Lancet* [Internet].
17 2013 [cited 2014 Jan 20];381:1371–9. Available from:
18 <http://www.ncbi.nlm.nih.gov/pubmed/23453885>
- 19 8. Lee SH, Ripke S, Neale BM, Faraone S V, Purcell SM, Perlis RH, et al. Genetic
20 relationship between five psychiatric disorders estimated from genome-wide SNPs. *Nat.*
21 *Genet.* [Internet]. 2013 [cited 2014 Jan 21];45:984–94. Available from:
22 <http://www.ncbi.nlm.nih.gov/pubmed/23933821>

- 1 9. Jääskeläinen E, Juola P, Hirvonen N, McGrath JJ, Saha S, Isohanni M, et al. A
2 systematic review and meta-analysis of recovery in schizophrenia. *Schizophr. Bull.*
3 2013;39:1296–306.
- 4 10. Hwang Y, Kim J, Shin JY, Kim JI, Seo JS, Webster MJ, et al. Gene expression
5 profiling by mRNA sequencing reveals increased expression of immune/inflammation-
6 related genes in the hippocampus of individuals with schizophrenia. *Transl. Psychiatry.*
7 2013;3:e321.
- 8 11. Kohen R, Dobra A, Tracy JH, Haugen E. Transcriptome profiling of human
9 hippocampus dentate gyrus granule cells in mental illness. *Transl. Psychiatry.*
10 2014;4:e366.
- 11 12. Akula N, Barb J, Jiang X, Wendland JR, Choi KH, Sen SK, et al. RNA-sequencing of
12 the brain transcriptome implicates dysregulation of neuroplasticity, circadian rhythms
13 and GTPase binding in bipolar disorder. *Mol. Psychiatry* [Internet]. 2014 [cited 2015
14 May 27];19:1179–85. Available from: <http://www.ncbi.nlm.nih.gov/pubmed/24393808>
- 15 13. Darby MM, Yolken RH, Sabunciyan S. Consistently altered expression of gene sets
16 in postmortem brains of individuals with major psychiatric disorders. *Transl. Psychiatry*
17 [Internet]. 2016 [cited 2016 Oct 7];6:e890. Available from:
18 <http://www.ncbi.nlm.nih.gov/pubmed/27622934>
- 19 14. Fromer M, Roussos P, Sieberts SK, Johnson JS, Kavanagh DH, Perumal TM, et al.
20 Gene expression elucidates functional impact of polygenic risk for schizophrenia. *Nat.*
21 *Neurosci.* [Internet]. 2016 [cited 2016 Oct 7]; Available from:
22 <http://www.ncbi.nlm.nih.gov/pubmed/27668389>

- 1 15. Olsen CM. Natural rewards, neuroplasticity, and non-drug addictions.
2 Neuropharmacology [Internet]. 2011 [cited 2015 Jun 17];61:1109–22. Available from:
3 [http://www.pubmedcentral.nih.gov/articlerender.fcgi?artid=3139704&tool=pmcentrez&re](http://www.pubmedcentral.nih.gov/articlerender.fcgi?artid=3139704&tool=pmcentrez&rendertype=abstract)
4 [ndertype=abstract](http://www.pubmedcentral.nih.gov/articlerender.fcgi?artid=3139704&tool=pmcentrez&rendertype=abstract)
- 5 16. Wenzel JM, Rauscher NA, Cheer JF, Oleson EB. A role for phasic dopamine
6 release within the nucleus accumbens in encoding aversion: a review of the
7 neurochemical literature. ACS Chem. Neurosci. [Internet]. 2015 [cited 2015 Aug
8 20];6:16–26. Available from: <http://www.ncbi.nlm.nih.gov/pubmed/25491156>
- 9 17. Evans SJ, Choudary P V, Vawter MP, Li J, Meador-Woodruff JH, Lopez JF, et al.
10 DNA microarray analysis of functionally discrete human brain regions reveals divergent
11 transcriptional profiles. Neurobiol. Dis. [Internet]. 2003 [cited 2015 Apr 18];14:240–50.
12 Available from:
13 [http://www.pubmedcentral.nih.gov/articlerender.fcgi?artid=3098567&tool=pmcentrez&re](http://www.pubmedcentral.nih.gov/articlerender.fcgi?artid=3098567&tool=pmcentrez&rendertype=abstract)
14 [ndertype=abstract](http://www.pubmedcentral.nih.gov/articlerender.fcgi?artid=3098567&tool=pmcentrez&rendertype=abstract)
- 15 18. Li JZ, Vawter MP, Walsh DM, Tomita H, Evans SJ, Choudary P V, et al. Systematic
16 changes in gene expression in postmortem human brains associated with tissue pH and
17 terminal medical conditions. Hum. Mol. Genet. [Internet]. 2004 [cited 2015 Apr
18 18];13:609–16. Available from: <http://www.ncbi.nlm.nih.gov/pubmed/14734628>
- 19 19. Jones EG, Hendry SH, Liu XB, Hodgins S, Potkin SG, Tourtellotte WW. A method
20 for fixation of previously fresh-frozen human adult and fetal brains that preserves
21 histological quality and immunoreactivity. J. Neurosci. Methods [Internet]. 1992 [cited
22 2017 Feb 4];44:133–44. Available from: <http://www.ncbi.nlm.nih.gov/pubmed/1282187>
- 23 20. Johnston NL, Cervenak J, Shore AD, Torrey EF, Yolken RH, Cerevna J.

- 1 Multivariate analysis of RNA levels from postmortem human brains as measured by
- 2 three different methods of RT-PCR. Stanley Neuropathology Consortium. *J. Neurosci.*
- 3 *Methods* [Internet]. 1997 [cited 2017 Feb 4];77:83–92. Available from:
- 4 <http://www.ncbi.nlm.nih.gov/pubmed/9402561>

- 5 21. Gertz J, Varley KE, Davis NS, Baas BJ, Goryshin IY, Vaidyanathan R, et al.
- 6 Transposase mediated construction of RNA-seq libraries. *Genome Res.* 2012;22:134–
- 7 41.

- 8 22. Alonso A, Lasseigne BN, Williams K, Nielsen J, Ramaker RC, Hardigan AA, et al.
- 9 aRNApipe: A balanced, efficient and distributed pipeline for processing RNA-seq data in
- 10 high performance computing environments. *Bioinformatics* [Internet]. 2017 [cited 2017
- 11 Feb 3];btx023. Available from:
- 12 <http://bioinformatics.oxfordjournals.org/lookup/doi/10.1093/bioinformatics/btx023>

- 13 23. Dobin A, Davis CA, Schlesinger F, Drenkow J, Zaleski C, Jha S, et al. STAR:
- 14 ultrafast universal RNA-seq aligner. *Bioinformatics* [Internet]. 2013 [cited 2017 Feb
- 15 3];29:15–21. Available from: <http://www.ncbi.nlm.nih.gov/pubmed/23104886>

- 16 24. Love MI, Huber W, Anders S. Moderated estimation of fold change and dispersion
- 17 for RNA-seq data with DESeq2. *Genome Biol.* [Internet]. 2014 [cited 2014 Dec
- 18 23];15:550. Available from:
- 19 [http://www.pubmedcentral.nih.gov/articlerender.fcgi?artid=4302049&tool=pmcentrez&re](http://www.pubmedcentral.nih.gov/articlerender.fcgi?artid=4302049&tool=pmcentrez&rendertype=abstract)
- 20 [ndertype=abstract](http://www.pubmedcentral.nih.gov/articlerender.fcgi?artid=4302049&tool=pmcentrez&rendertype=abstract)

- 21 25. Kim JH, Karnovsky A, Mahavisno V, Weymouth T, Pande M, Dolinoy DC, et al.
- 22 LRpath analysis reveals common pathways dysregulated via DNA methylation across
- 23 cancer types. *BMC Genomics* [Internet]. 2012 [cited 2015 Aug 20];13:526. Available

- 1 from:
- 2 [http://www.pubmedcentral.nih.gov/articlerender.fcgi?artid=3505188&tool=pmcentrez&re](http://www.pubmedcentral.nih.gov/articlerender.fcgi?artid=3505188&tool=pmcentrez&rendertype=abstract)
- 3 [ndertype=abstract](http://www.pubmedcentral.nih.gov/articlerender.fcgi?artid=3505188&tool=pmcentrez&rendertype=abstract)
- 4 26. Isserlin R, Merico D, Voisin V, Bader GD. Enrichment Map - a Cytoscape app to
- 5 visualize and explore OMICs pathway enrichment results. *F1000Research* [Internet].
- 6 2014 [cited 2015 Aug 20];3:141. Available from:
- 7 [http://www.pubmedcentral.nih.gov/articlerender.fcgi?artid=4103489&tool=pmcentrez&re](http://www.pubmedcentral.nih.gov/articlerender.fcgi?artid=4103489&tool=pmcentrez&rendertype=abstract)
- 8 [ndertype=abstract](http://www.pubmedcentral.nih.gov/articlerender.fcgi?artid=4103489&tool=pmcentrez&rendertype=abstract)
- 9 27. Darmanis S, Sloan S a., Zhang Y, Enge M, Caneda C, Shuer LM, et al. A survey of
- 10 human brain transcriptome diversity at the single cell level. *Proc. Natl. Acad. Sci.*
- 11 2015;201507125.
- 12 28. Zhang Y, Sloan SA, Clarke LE, Caneda C, Plaza CA, Blumenthal PD, et al.
- 13 Purification and Characterization of Progenitor and Mature Human Astrocytes Reveals
- 14 Transcriptional and Functional Differences with Mouse. *Neuron* [Internet]. 2015 [cited
- 15 2015 Dec 16];89:37–53. Available from:
- 16 <http://www.sciencedirect.com/science/article/pii/S0896627315010193>
- 17 29. Zhang Y, Chen K, Sloan SA, Bennett ML, Scholze AR, O’Keeffe S, et al. An RNA-
- 18 Sequencing Transcriptome and Splicing Database of Glia, Neurons, and Vascular Cells
- 19 of the Cerebral Cortex. *J. Neurosci.* [Internet]. 2014 [cited 2014 Sep 5];34:11929–47.
- 20 Available from:
- 21 [http://www.pubmedcentral.nih.gov/articlerender.fcgi?artid=4152602&tool=pmcentrez&re](http://www.pubmedcentral.nih.gov/articlerender.fcgi?artid=4152602&tool=pmcentrez&rendertype=abstract)
- 22 [ndertype=abstract](http://www.pubmedcentral.nih.gov/articlerender.fcgi?artid=4152602&tool=pmcentrez&rendertype=abstract)
- 23 30. Gong T, Szustakowski JD. DeconRNASeq: a statistical framework for deconvolution

- 1 of heterogeneous tissue samples based on mRNA-Seq data. *Bioinformatics* [Internet].
2 Oxford University Press; 2013 [cited 2017 May 25];29:1083–5. Available from:
3 [https://academic.oup.com/bioinformatics/article-](https://academic.oup.com/bioinformatics/article-lookup/doi/10.1093/bioinformatics/btt090)
4 [lookup/doi/10.1093/bioinformatics/btt090](https://academic.oup.com/bioinformatics/article-lookup/doi/10.1093/bioinformatics/btt090)
- 5 31. Dunn WB, Broadhurst D, Begley P, Zelena E, Francis-McIntyre S, Anderson N, et
6 al. Procedures for large-scale metabolic profiling of serum and plasma using gas
7 chromatography and liquid chromatography coupled to mass spectrometry. *Nat. Protoc.*
8 [Internet]. 2011 [cited 2015 Dec 28];6:1060–83. Available from:
9 <http://www.ncbi.nlm.nih.gov/pubmed/21720319>
- 10 32. Hummel J, Strehmel N, Selbig J, Walther D, Kopka J. Decision tree supported
11 substructure prediction of metabolites from GC-MS profiles. *Metabolomics* [Internet].
12 2010 [cited 2016 Feb 3];6:322–33. Available from:
13 [http://www.pubmedcentral.nih.gov/articlerender.fcgi?artid=2874469&tool=pmcentrez&re](http://www.pubmedcentral.nih.gov/articlerender.fcgi?artid=2874469&tool=pmcentrez&rendertype=abstract)
14 [ndertype=abstract](http://www.pubmedcentral.nih.gov/articlerender.fcgi?artid=2874469&tool=pmcentrez&rendertype=abstract)
- 15 33. Castillo S, Mattila I, Miettinen J, Orešič M, Hyötyläinen T. Data analysis tool for
16 comprehensive two-dimensional gas chromatography/time-of-flight mass spectrometry.
17 *Anal. Chem.* [Internet]. 2011 [cited 2015 Aug 24];83:3058–67. Available from:
18 <http://www.ncbi.nlm.nih.gov/pubmed/21434611>
- 19 34. Subramanian A, Tamayo P, Mootha VK, Mukherjee S, Ebert BL, Gillette M a, et al.
20 Gene set enrichment analysis: a knowledge-based approach for interpreting genome-
21 wide expression profiles. *Proc. Natl. Acad. Sci. U. S. A.* [Internet]. 2005;102:15545–50.
22 Available from: <http://www.ncbi.nlm.nih.gov/pubmed/16199517>
- 23 35. Network and Pathway Analysis Subgroup of Psychiatric Genomics Consortium.

- 1 Psychiatric genome-wide association study analyses implicate neuronal, immune and
2 histone pathways. *Nat. Neurosci.* [Internet]. 2015 [cited 2017 Feb 16];18:199–209.
3 Available from: <http://www.nature.com/doi/10.1038/nn.3922>
- 4 36. Vita A, De Peri L, Deste G, Sacchetti E. Progressive loss of cortical gray matter in
5 schizophrenia: a meta-analysis and meta-regression of longitudinal MRI studies. *Transl.*
6 *Psychiatry* [Internet]. Nature Publishing Group; 2012;2:e190. Available from:
7 [http://www.pubmedcentral.nih.gov/articlerender.fcgi?artid=3565772&tool=pmcentrez&re](http://www.pubmedcentral.nih.gov/articlerender.fcgi?artid=3565772&tool=pmcentrez&rendertype=abstract)
8 [ndertype=abstract](http://www.pubmedcentral.nih.gov/articlerender.fcgi?artid=3565772&tool=pmcentrez&rendertype=abstract)
- 9 37. Berretta S, Pantazopoulos H, Lange N. Neuron numbers and volume of the
10 amygdala in subjects diagnosed with bipolar disorder or schizophrenia. *Biol. Psychiatry*
11 [Internet]. 2007 [cited 2017 Feb 2];62:884–93. Available from:
12 <http://linkinghub.elsevier.com/retrieve/pii/S0006322307003575>
- 13 38. Thompson M, Weickert CS, Wyatt E, Webster MJ. Decreased glutamic acid
14 decarboxylase(67) mRNA expression in multiple brain areas of patients with
15 schizophrenia and mood disorders. *J. Psychiatr. Res.* [Internet]. 2009 [cited 2015 May
16 14];43:970–7. Available from: <http://www.ncbi.nlm.nih.gov/pubmed/19321177>
- 17 39. Skelly DA, Merrihew GE, Riffle M, Connelly CF, Kerr EO, Johansson M, et al.
18 Integrative phenomics reveals insight into the structure of phenotypic diversity in
19 budding yeast. *Genome Res.* [Internet]. 2013 [cited 2015 Aug 20];23:1496–504.
20 Available from:
21 [http://www.pubmedcentral.nih.gov/articlerender.fcgi?artid=3759725&tool=pmcentrez&re](http://www.pubmedcentral.nih.gov/articlerender.fcgi?artid=3759725&tool=pmcentrez&rendertype=abstract)
22 [ndertype=abstract](http://www.pubmedcentral.nih.gov/articlerender.fcgi?artid=3759725&tool=pmcentrez&rendertype=abstract)
- 23 40. Kim S, Hwang Y, Webster MJ, Lee D. Differential activation of immune/inflammatory

- 1 response-related co-expression modules in the hippocampus across the major
2 psychiatric disorders. *Mol. Psychiatry* [Internet]. Nature Publishing Group; 2015;1–10.
3 Available from: <http://www.nature.com/doi/10.1038/mp.2015.79>
- 4 41. Sequeira A, Morgan L, Walsh DM, Cartagena PM, Choudary P, Li J, et al. Gene
5 expression changes in the prefrontal cortex, anterior cingulate cortex and nucleus
6 accumbens of mood disorders subjects that committed suicide. *PLoS One* [Internet].
7 2012 [cited 2014 Jul 15];7:e35367. Available from:
8 [http://www.pubmedcentral.nih.gov/articlerender.fcgi?artid=3340369&tool=pmcentrez&re](http://www.pubmedcentral.nih.gov/articlerender.fcgi?artid=3340369&tool=pmcentrez&rendertype=abstract)
9 [ndertype=abstract](http://www.pubmedcentral.nih.gov/articlerender.fcgi?artid=3340369&tool=pmcentrez&rendertype=abstract)
- 10 42. Sorenson SB. Gender disparities in injury mortality: Consistent, persistent, and
11 larger than you'd think. *Am. J. Public Health*. 2011;101:353–8.
- 12 43. Aubin H-J, Rollema H, Svensson TH, Winterer G. Smoking, quitting, and psychiatric
13 disease: A review. *Neurosci. Biobehav. Rev.* [Internet]. 2012 [cited 2017 Feb 3];36:271–
14 84. Available from: <http://www.ncbi.nlm.nih.gov/pubmed/21723317>
- 15 44. Wolock SL, Yates A, Petrill SA, Bohland JW, Blair C, Li N, et al. Gene x smoking
16 interactions on human brain gene expression: finding common mechanisms in
17 adolescents and adults. *J. Child Psychol. Psychiatry.* [Internet]. NIH Public Access;
18 2013 [cited 2017 Feb 3];54:1109–19. Available from:
19 <http://www.ncbi.nlm.nih.gov/pubmed/23909413>
- 20 45. Weissman DH, Gopalakrishnan a., Hazlett CJ, Woldorff MG. Dorsal anterior
21 cingulate cortex resolves conflict from distracting stimuli by boosting attention toward
22 relevant events. *Cereb. Cortex*. 2005;15:229–37.

- 1 46. Paus T. Primate anterior cingulate cortex: where motor control, drive and cognition
2 interface. *Nat. Rev. Neurosci.* 2001;2:417–24.
- 3 47. Carter CS, Braver TS, Barch DM, Botvinick MM, Noll D, Cohen JD. Anterior
4 cingulate cortex, error detection, and the online monitoring of performance. *Science.*
5 1998;280:747–9.
- 6 48. Woo T-UW, Kim AM, Viscidi E. Disease-specific alterations in glutamatergic
7 neurotransmission on inhibitory interneurons in the prefrontal cortex in schizophrenia.
8 *Brain Res.* [Internet]. 2008 [cited 2015 May 27];1218:267–77. Available from:
9 [http://www.pubmedcentral.nih.gov/articlerender.fcgi?artid=2665281&tool=pmcentrez&re](http://www.pubmedcentral.nih.gov/articlerender.fcgi?artid=2665281&tool=pmcentrez&rendertype=abstract)
10 [ndertype=abstract](http://www.pubmedcentral.nih.gov/articlerender.fcgi?artid=2665281&tool=pmcentrez&rendertype=abstract)
- 11 49. Yamada K, Gerber DJ, Iwayama Y, Ohnishi T, Ohba H, Toyota T, et al. Genetic
12 analysis of the calcineurin pathway identifies members of the EGR gene family,
13 specifically EGR3, as potential susceptibility candidates in schizophrenia. *Proc. Natl.*
14 *Acad. Sci. U. S. A.* [Internet]. 2007 [cited 2015 Aug 19];104:2815–20. Available from:
15 [http://www.pubmedcentral.nih.gov/articlerender.fcgi?artid=1815264&tool=pmcentrez&re](http://www.pubmedcentral.nih.gov/articlerender.fcgi?artid=1815264&tool=pmcentrez&rendertype=abstract)
16 [ndertype=abstract](http://www.pubmedcentral.nih.gov/articlerender.fcgi?artid=1815264&tool=pmcentrez&rendertype=abstract)
- 17 50. Pérez-Santiago J, Diez-Alarcia R, Callado LF, Zhang JX, Chana G, White CH, et al.
18 A combined analysis of microarray gene expression studies of the human prefrontal
19 cortex identifies genes implicated in schizophrenia. *J. Psychiatr. Res.* [Internet].
20 Elsevier; 2012 [cited 2017 Feb 3];46:1464–74. Available from:
21 <http://www.ncbi.nlm.nih.gov/pubmed/22954356>
- 22 51. Zhang L, Cho J, Ptak D, Leung YF. The Role of *egr1* in Early Zebrafish
23 Retinogenesis. *PLoS One.* 2013;8:1–11.

- 1 52. Baumgärtel K, Genoux D, Welzl H, Tweedie-Cullen RY, Koshibu K, Livingstone-
2 Zatchej M, et al. Control of the establishment of aversive memory by calcineurin and
3 Zif268. *Nat. Neurosci.* [Internet]. 2008 [cited 2017 Feb 3];11:572–8. Available from:
4 <http://www.nature.com/doi/10.1038/nn.2113>
- 5 53. Bruins Slot LA, Lestienne F, Grevoz-Barret C, Newman-Tancredi A, Cussac D.
6 F15063, a potential antipsychotic with dopamine D(2)/D(3) receptor antagonist and 5-
7 HT(1A) receptor agonist properties: influence on immediate-early gene expression in rat
8 prefrontal cortex and striatum. *Eur. J. Pharmacol.* [Internet]. 2009 [cited 2017 Feb
9 3];620:27–35. Available from:
10 <http://linkinghub.elsevier.com/retrieve/pii/S0014299909006906>
- 11 54. Xu Y, Yue W, Shugart YY, Li S, Cai L, Li Q, et al. Exploring transcription factors-
12 microRNAs co-regulation networks in schizophrenia. *Schizophr. Bull.* 2016;42:1037–45.
- 13 55. Koldamova R, Schug J, Lefterova M, Cronican AA, Fitz NF, Davenport FA, et al.
14 Genome-wide approaches reveal EGR1-controlled regulatory networks associated with
15 neurodegeneration. *Neurobiol. Dis.* [Internet]. 2014 [cited 2017 Feb 26];63:107–14.
16 Available from: <http://linkinghub.elsevier.com/retrieve/pii/S0969996113003173>
- 17 56. Fromer M, Pocklington AJ, Kavanagh DH, Williams HJ, Dwyer S, Gormley P, et al.
18 De novo mutations in schizophrenia implicate synaptic networks. *Nature* [Internet]. 2014
19 [cited 2014 Jul 10];506:179–84. Available from:
20 [http://www.pubmedcentral.nih.gov/articlerender.fcgi?artid=4237002&tool=pmcentrez&re
21 ndertype=abstract](http://www.pubmedcentral.nih.gov/articlerender.fcgi?artid=4237002&tool=pmcentrez&rendertype=abstract)
- 22 57. Fromer M, Roussos P, Sieberts SK, Johnson JS, Kavanagh DH, Perumal TM, et al.
23 Gene expression elucidates functional impact of polygenic risk for schizophrenia. *Nat.*

1 Neurosci. [Internet]. 2016;19:1442–53. Available from:
2 <http://www.nature.com/doifinder/10.1038/nn.4399>
3 58. Guillozet-Bongaarts AL, Hyde TM, Dalley RA, Hawrylycz MJ, Henry A, Hof PR, et al.
4 Altered gene expression in the dorsolateral prefrontal cortex of individuals with
5 schizophrenia. Mol. Psychiatry [Internet]. Nature Publishing Group; 2014 [cited 2017
6 Feb 3];19:478–85. Available from: <http://www.nature.com/doifinder/10.1038/mp.2013.30>
7

8 **Figure Legends**

9 **Figure 1.** (A) Histograms of case vs. control differential expression (DESeq2 p-values)
10 for SZ (red), BPD (blue), and MDD (green) in each brain region assayed. A minimum
11 DESeq2 base mean of 10 was required for inclusion. (B) Pairwise spearman
12 correlations of \log_2 fold gene expression changes between each disorder and CTL in
13 each brain region. Circle sizes are scaled to reflect absolute Spearman correlations.
14 (C) Venn diagram showing overlap of genes differentially expressed between SZ (red),
15 BPD (blue), MDD (green) vs. CTL at p -value <0.05 in the AnCg. (D) \log_2 fold expression
16 change correlation of 87 genes with $FDR<0.05$ comparing SZ and CTL (AnCg) in the
17 Pritzker dataset with the SNCID dataset (Spearman coefficient=0.812, p -value <0.0001).
18 Genes differentially expressed at an $FDR<0.05$ in both cohorts are identified with red
19 circles. (E) Hierarchical clustering 27 SZ and 26 CTL tissues in the SNCID dataset
20 using variance-stabilized expression of 1003 genes differentially expressed between SZ
21 and CTL in the AnCg (uncorrected p -value <0.05) in the Pritzker dataset. CTL (black),
22 SZ (red), lowly expressed genes (blue pixels), highly expressed genes (yellow pixels).

1 **Figure 2.** (A) Boxplots indicating relative expression of *EGR1* in the AnCg of SZ (red),
2 BPD (blue), MDD (green), and CTL (gray). (B) Correlation plot comparing RNA-seq
3 measured expression level of *EGR1* to qPCR measured expression in 10 SZ (red) and
4 10 CTL (black) patients. (C) Wilcox p-values resulting from comparing the degree of
5 differential expression (based on DESeq2 p-values) of genes whose TSS are within the
6 indicated distance to an *EGR1* binding sites compared to to genes whose TSSs are
7 greater than the indicated threshold.

8 **Figure 3.** Boxplots indicating z-scored neuron- (A) and astrocyte- (B) specific
9 expression indices in the AnCg for SZ (red), BPD (blue), MDD (green), and CTL (gray)
10 individuals. (C) Correlation plot comparing the \log_2 expression fold change between SZ
11 and CTL patients in the AnCg (X-axis) and the \log_2 fold change in gene expression from
12 dissected neuron populations compared to all other dissected brain cell types
13 (astrocytes, oligodendrocytes, endothelial cells, and microglia) for each transcript
14 measured by Zhang et al.

15 **Figure 4.** Hierarchical clustering of SZ (red), BPD (blue), MDD (green), and CTL
16 (black) individuals using the top ten most significant metabolites for each case-control
17 comparison (for a total of 30 metabolites). (B) Boxplots indicating z-scored GABA
18 metabolite levels. (C) Boxplots indicating relative expression of GAD1 and GAD2
19 enzymes in the AnCg of SZ (red) and CTL (gray) patients. (D) Correlation plot
20 comparing average GAD1 and GAD2 expression and the GABA/Glutamate metabolite
21 level ratio in the AnCg of SZ (red) and CTL (black) individuals.

22 **Supplementary Figure Legends**

1 **Figure S1.** A) Principal components analysis of all 281 brain tissues. AnCg (red
2 squares), DLPFC (blue triangles), nAcc (green circles). B) Principal components
3 analysis of all 281 brain tissues. CTL (gray squares), BPD (blue triangles), MDD (green
4 circles), SZ (red triangles). (C) Principal components analysis of all 281 brain tissues
5 after correcting RNA-seq data for alignment quality. CTL (gray squares), BPD (blue
6 triangles), MDD (green circles), SZ (red triangles).

7 **Figure S2.** Principal components analysis of all AnCg (A,D), DLPFC (B,E), and nAcc
8 (C,F) samples before (A-C) and after (D-F) correction for RNA-seq alignment quality.
9 (G-I) PC1 values in CTL (gray), BPD (blue), MDD (green), and SZ (red) patients pre-
10 and post-RNA-seq alignment quality correction in the AnCg (G), DLPFC (H), and nAcc
11 (I).

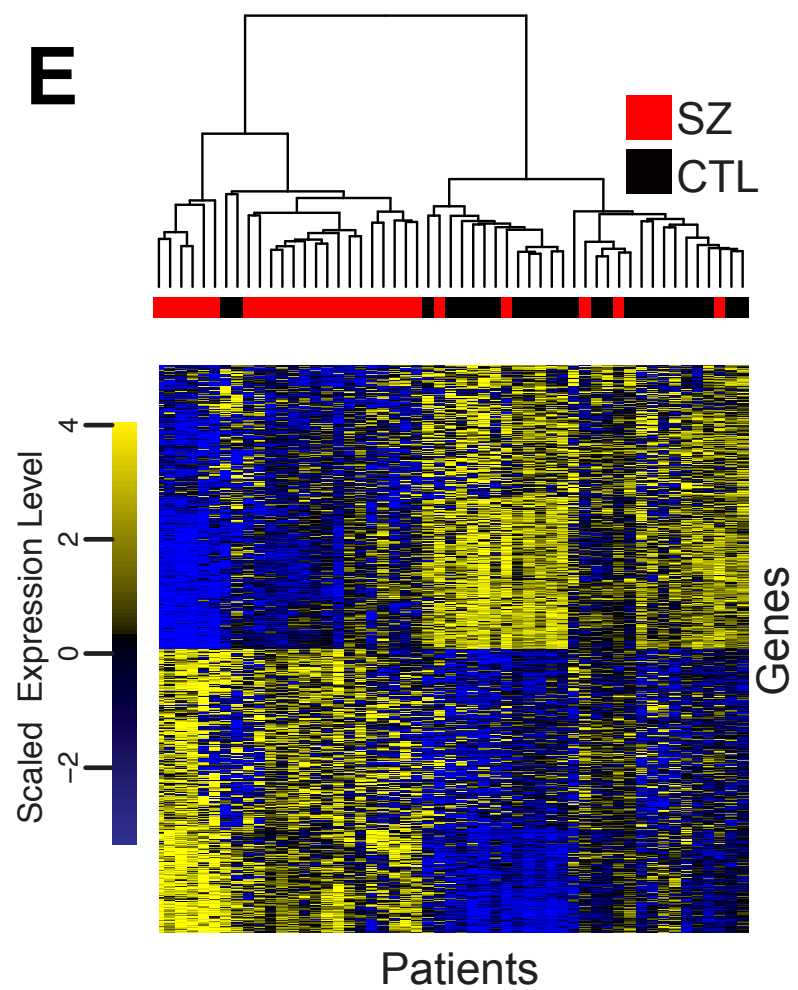
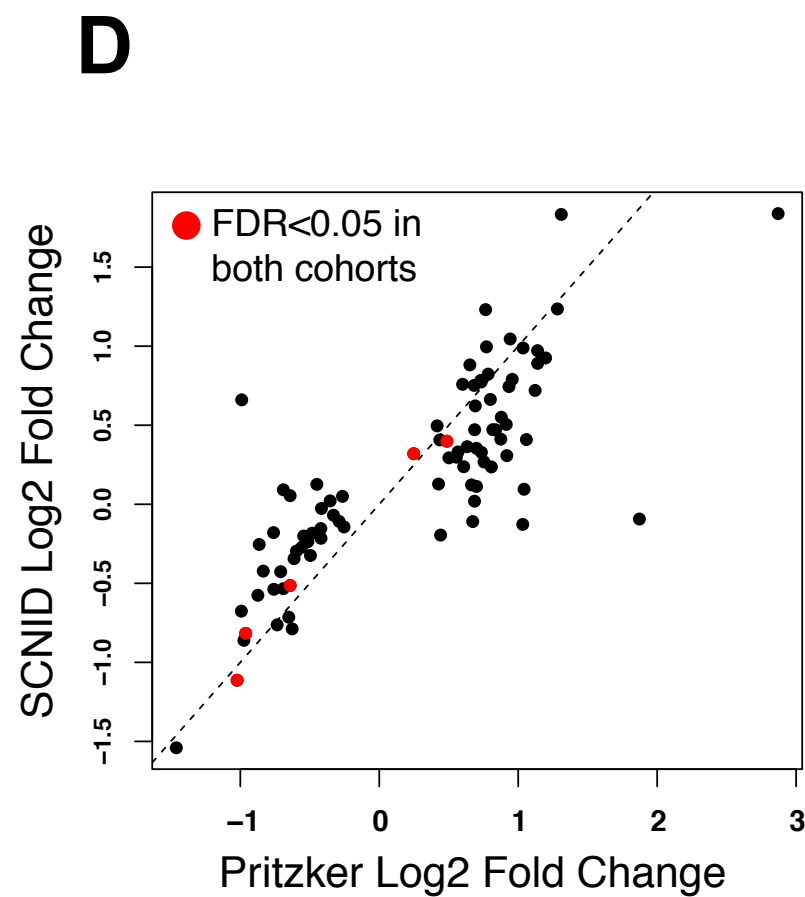
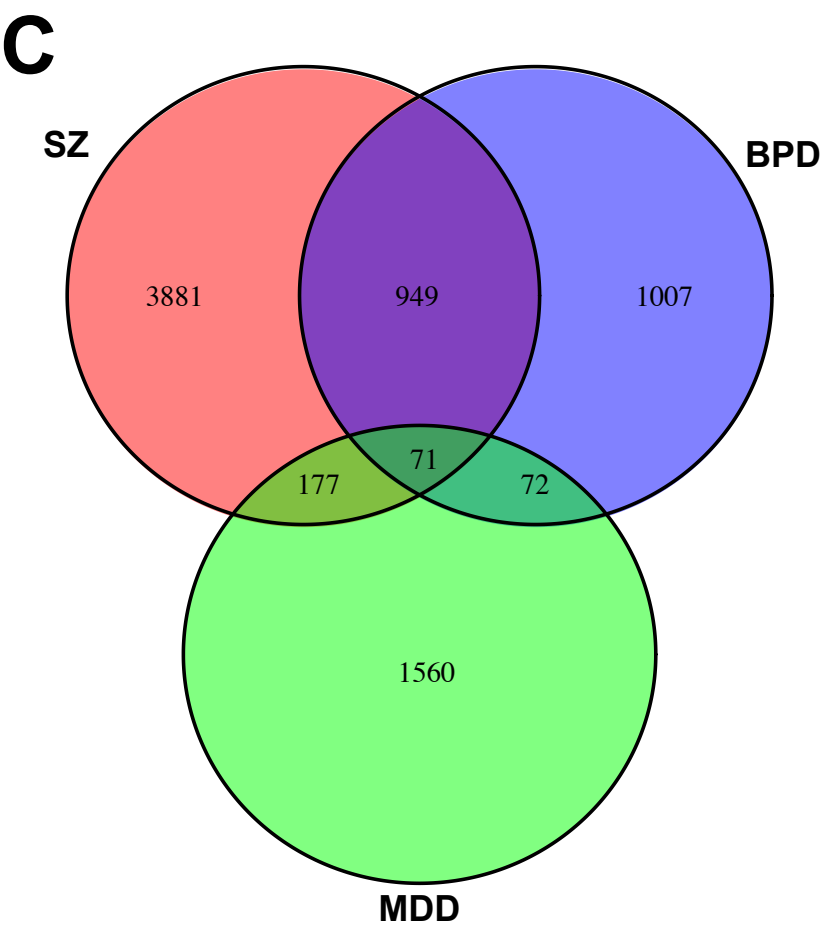
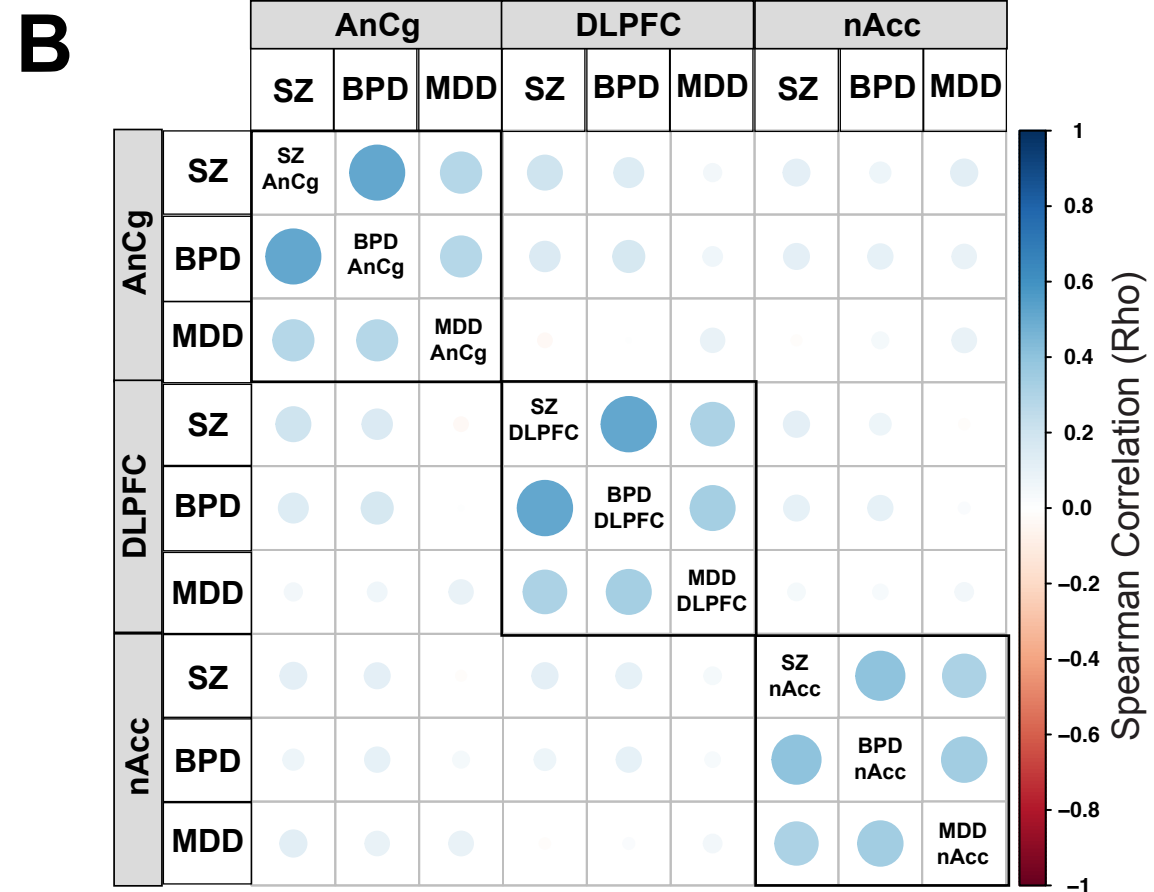
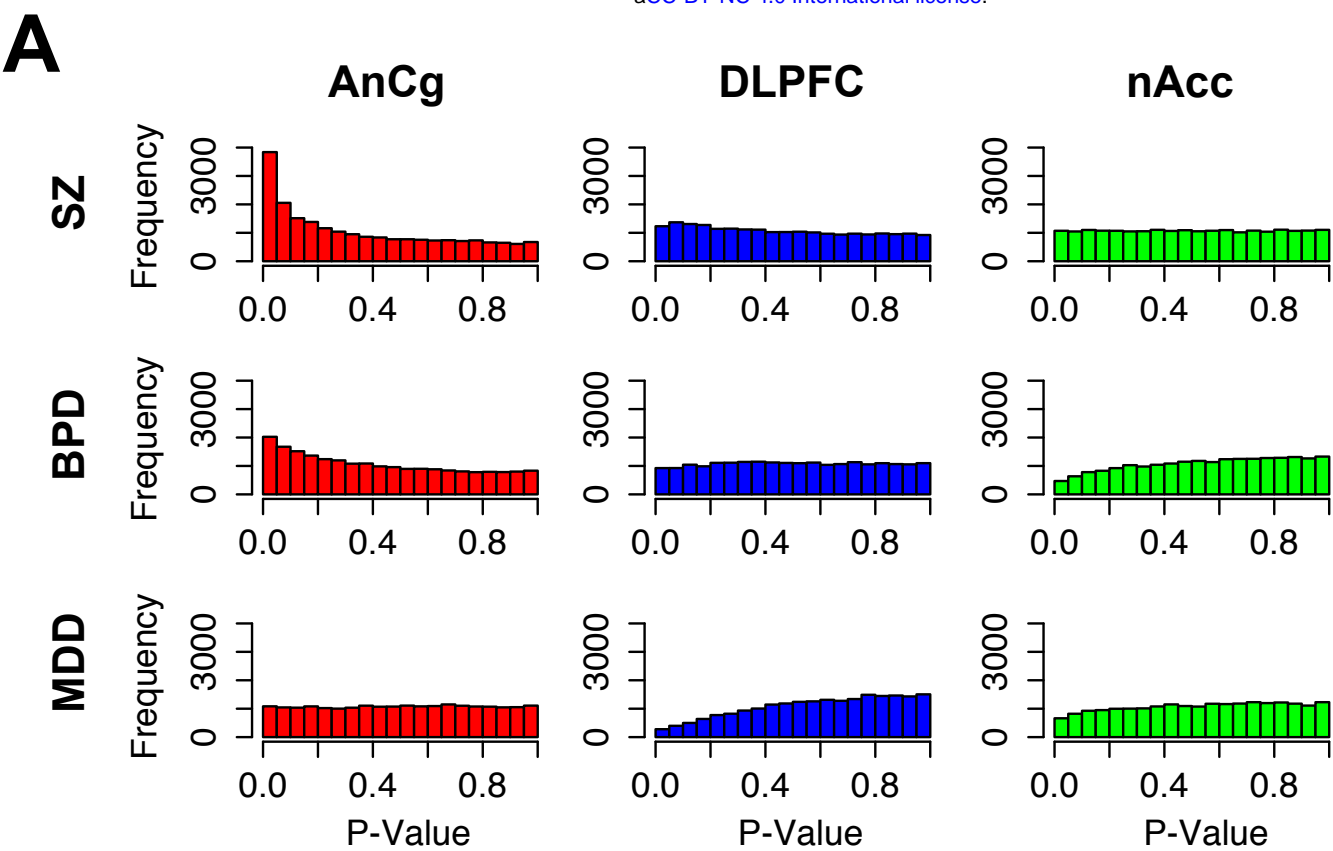
12 **Figure S3.** GO-term analysis for genes differentially expressed in SZ vs. CTL in AnCg
13 (FDR<0.05). Up-regulation (red circles), down-regulation (blue circles).

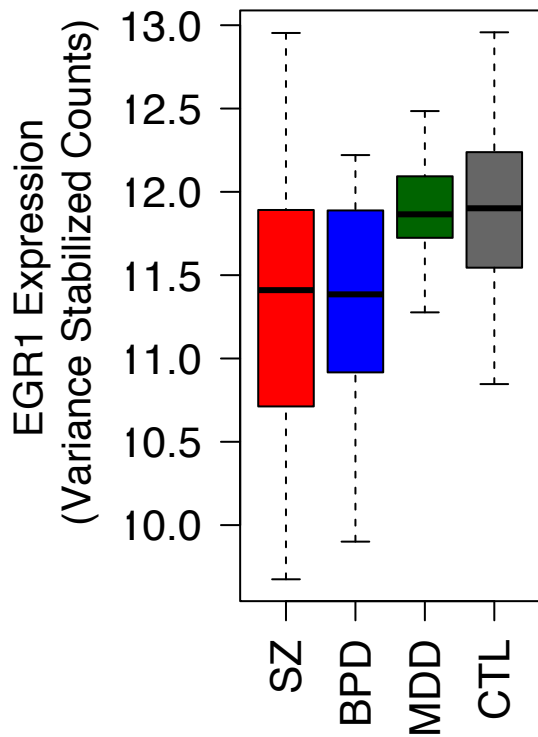
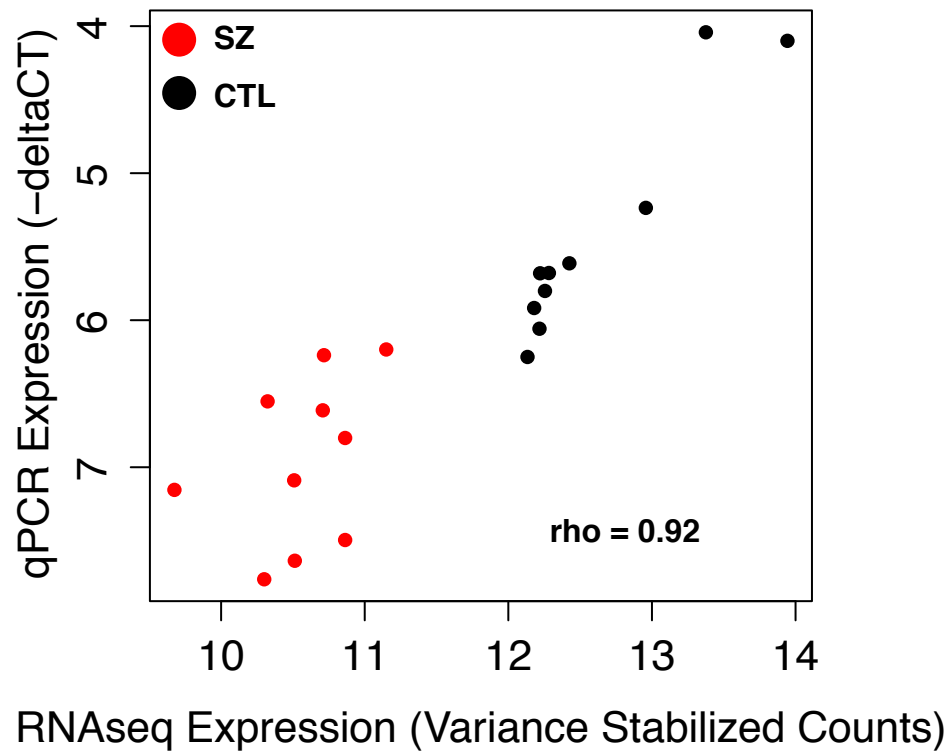
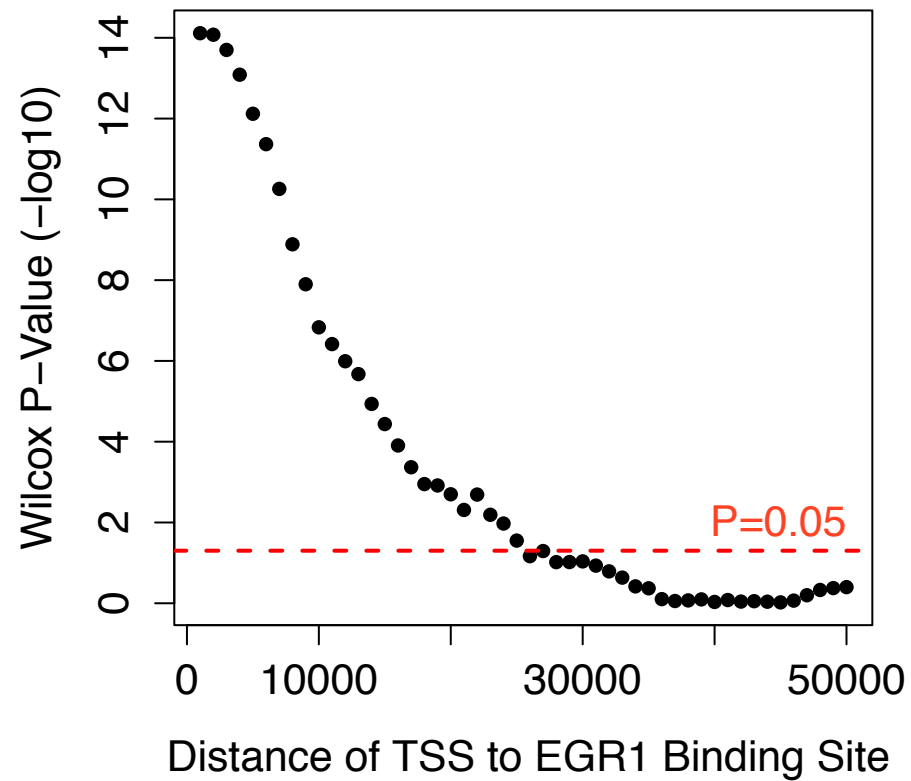
14 **Figure S4.** Using cell-type specific index based on single cell sequencing, we
15 calculated the index for purified populations of (A) neurons, (B) astrocytes, (C)
16 oligodendrocytes, (D) microglia, and (E) endothelial cells. In all cases the calculated
17 indexes were specific to the purified population (F) Neuron and astrocyte indices were
18 used to predict the proportion of each cell type in *in silico* mixed cell-type populations.
19 (G) Compared to the Darmanis et al. indexes, 10,000 randomly generated gene sets do
20 not predict cell type proportions. Mean values with standard deviation are plotted (H, I)
21 Histogram of mean squared error of null index cell type proportion predictions for mixed
22 neuron and astrocyte transcriptomes with Darmanis et al. gene performance indicated
23 in red. The Darmanis gene set far outperforms any randomly generated gene sets.

1 **Figure S5.** Boxplots of endothelial (A), microglia (B), and oligodendrocyte (C) cell type
2 indices in SZ (red), BPD (blue), MDD (green), and CTL (gray) individuals using indices
3 derived from Darmanis et al.

4 **Figure S6.** (A,B) Estimated neuron (A) and astrocyte (B) cell type proportions using the
5 deconRNAseq deconvolution algorithm in SZ, BPD, MDD, and CTL individuals. (C)
6 Volcano plot of cell type specific transcripts in the Darmanis et al. gene sets show
7 altered expression in SZ v CTL. Neuronal transcripts are enriched for loss of expression
8 and astrocyte-specific transcripts are enriched for increased expression (D,E)
9 Histograms representing the distribution of median log2 fold change for expression level
10 matched gene sets to neuron (D) and astrocyte (C) specific genes. Red lines indicate
11 median log2 fold change observed for neuron- and astrocyte-specific genes
12 respectively.

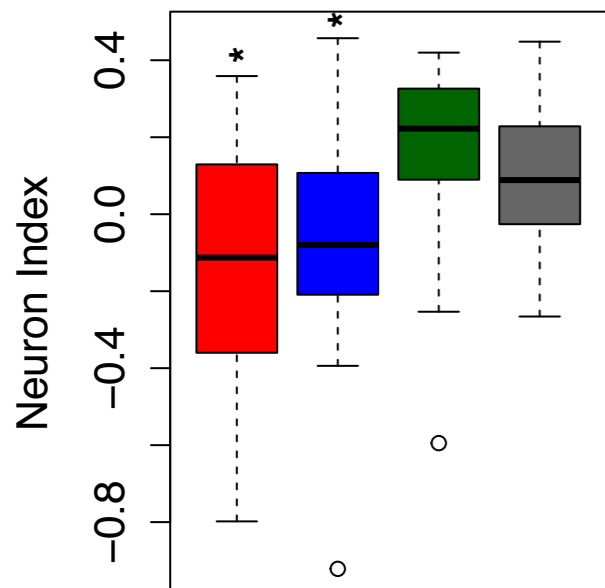
13 **Figure S7.** Integrated KEGG pathway analysis of metabolite and RNA-seq differences
14 between SZ and CTL patients. Top 10 pathways are shown for metabolite, gene and
15 combined analysis.



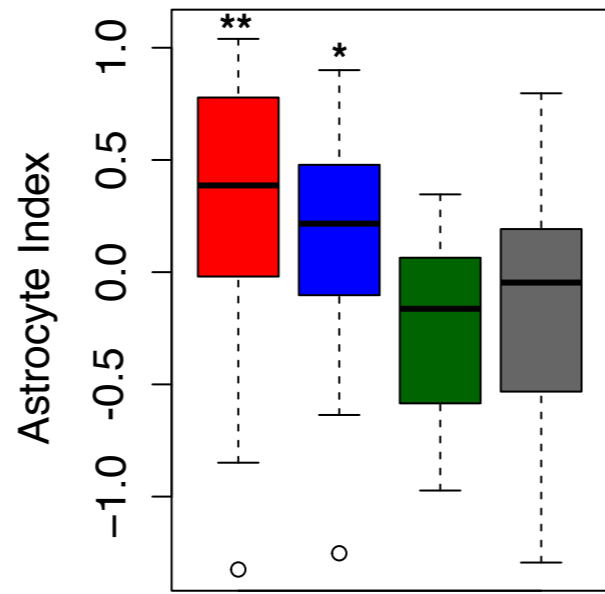
A**B****C**

A

Neuron Specific Expression

**B**

Astrocyte Specific Expression

**C**

Log2 Fold Enrichment in Neurons

